Influence of Nitrogen Dioxide Absorption on the Sulfite Oxidation Rate in the Presence of Oxygen: Online Raman Measurements

(article starts on next page)

Article

Influence of Nitrogen Dioxide Absorption on the Sulfite Oxidation Rate in the Presence of Oxygen: Online Raman Measurements

Jakob Johansson,* Jayangi D. Wagaarachchige, Fredrik Normann, Zulkifli Idris, Eirik R. Haugen, Maths Halstensen, Wathsala Jinadasa, Klaus J. Jens, and Klas Andersson

Read Online

ACCESS | Metrics & More | Article Recommendations | Supporting Information

ABSTRACT: The oxidation of sulfite(aq) is investigated by passing O_2, N_2, and NO_2 over a sulfite solution in a bubbling flask. The influence on sulfite oxidation of NO_2 absorption and the presence of thiosulfate (an oxidation inhibitor) is investigated. The experiment is focused on conditions relevant to a combined SO_2 and NO_2 industrial flue gas cleaning system. Liquid composition is measured in situ using Raman spectroscopy equipped with immersion probes. Regression models are developed to quantify SO_3^{2-}, HSO_3^{-}, $S_2O_3^{2-}$, SO_4^{2-}, NO_2^{-}, NO_3^{-}, and CO_3^{2-} also in mixtures of the mentioned chemicals. The results show that Raman spectroscopy is a possible method for liquid analysis of a NO_x/SO_x removal system. Speciation is successful within the limits of the experiment for most molecules. SO_4^{2-}, CO_3^{2-}, and $S_2O_3^{2-}$ are quantified with high certainty; SO_3^{2-} and HSO_3^{-} are quantified with some uncertainty and should be above 10 mM for quantitative measurements. NO_3^{-} concentration is below the limit of detection in the continuous experiments. The measured reaction rates of sulfite (SO_3^{2-}) and bisulfite (HSO_3^{-}) oxidation with O_2 are in agreement with the reviewed literature. Absorption of $NO_2(g)$ and the consequent formation of nitrite enhance sulfite oxidation. The addition of thiosulfate to the liquid reduces the rate of SO_3^{2-} oxidation by ∼90% while maintaining NO_2 absorption. The influence of $NO_2(g)$ and thiosulfate supports a previously proposed mechanism for sulfite oxidation via a radical chain mechanism.
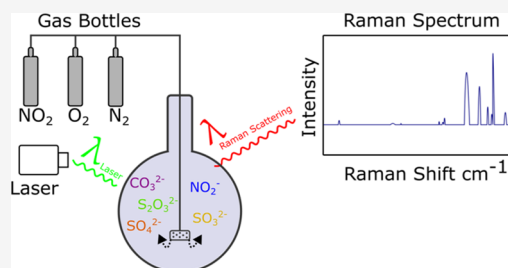
1. INTRODUCTION

The simultaneous absorption of sulfur dioxide (SO_2) and nitrogen oxides (NO_x) has been identified as an emerging technology with a large potential in industries where conventional flue gas cleaning is impractical, for different reasons. Common to the approaches of combined removal is that the nitric oxide (NO) is oxidized to NO_2 to increase the solubility. After the oxidation of NO to NO_2, NO_2 can be absorbed, together with SO_2, in a wet scrubber, similar to conventional wet flue gas desulfurization (WFGD). S(IV) ions (SO_3^{2-} and HSO_3^{-}) are crucial for the absorption of NO_2 to take place at a high rate.[1] S(IV) may be added as a salt or may be formed from absorbed $SO_2(g)$. In the absorption of NO_2, the S(IV) is oxidized to S(VI), and the NO_2 is absorbed and hydrolyzed to NO_2^{-}.[2] The oxidation of S(IV) can increase the absorption rate of SO_2 which has the benefit of removing SO_2 and NO_x in the same unit. However, sulfite has proven to oxidize at a much higher rate than can be explained by NO_2 absorption.[1] The addition of S(IV) salts to the liquid is conducted to maintain desirable NO_2 absorption levels. The S(IV) salt addition is associated with a cost, and the apparent kinetics of the sulfite oxidation is therefore of great interest to many researchers to better understand how the process can be controlled.

In Figure 1 a simplified schematic of the reaction paths possible when both $SO_2(g)$ and $NO_x(g)$ are present and in contact with an aqueous phase is shown. SO_2 absorption in
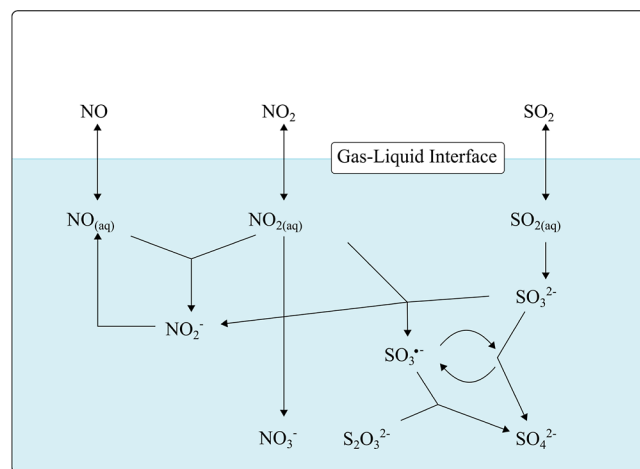

Figure 1. Schematic overview of the reaction paths used to describe the simultaneous absorption of NO_x and SO_x in an alkaline/neutral solution.

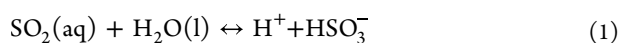water is equilibrium-controlled and leads to the formation of bisulfite and sulfite according to reactions 1 and 2, respectively[3−6]

$$SO_2(aq) + H_2O(l) \leftrightarrow H^+ + HSO_3^- \tag{1}$$

$$HSO_3^-(aq) \leftrightarrow H^+ + SO_3^{2-} \tag{2}$$

Absorption of NO_2 in water takes place according to either reactions 3 or 4, depending on the presence of NO and the pH level.[7−9]

$$2NO_2(aq) + H_2O(l) \rightarrow HNO_2(aq) + HNO_3(aq) \tag{3}$$

$$NO + NO_2 + H_2O \leftrightarrow 2HNO_2 \tag{4}$$

Nitrite, N(III), is inherently unstable, especially under acidic conditions, and it can decompose into NO and NO_2

$$2HNO_2(aq) \leftrightarrow NO(aq) + NO_2(aq) + H_2O \tag{5}$$
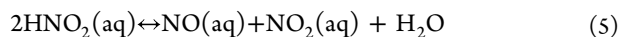
Several studies have shown that S(IV) is efficient at hydrolyzing $NO_2(aq)$ at a high rate according to reaction 6.[10−14]

$$2NO_2(aq) + SO_3^{2-} + H_2O(l) \rightarrow 2NO_2^- + SO_4^{2-} + 2H^+ \tag{6}$$
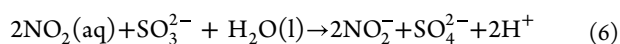
The SO_3^{2-} may also be oxidized by O_2 following reaction 7.

$$\frac{1}{2}O_2(aq) + SO_3^{2-} \rightarrow SO_4^{2-} \tag{7}$$
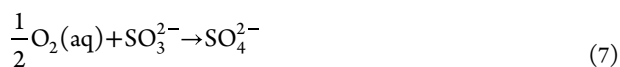
In experiments, it was found, as previously mentioned, that the oxidation of S(IV) progresses at a much higher rate than what is explained by reactions 6 and 7 alone. Nash[2] proposed that a radical-initiated chain of reactions was initiated by reaction 6 and rather progressed through reaction 8 where a sulfite radical was formed. This set of reactions enables depletion of SO_3^{2-} with only a single SO_3^{2-} radical formed if O_2 is present.

$$NO_2(aq) + SO_3^{2-} \rightarrow NO_2^- + SO_3^{•-} \tag{8}$$
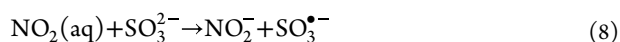
To break this chain of reactions a radical scavenger can be added to the liquid, which enables an alternative terminating step. One example of such a scavenger is $S_2O_3^{2-}$. Shen and Rochelle[15] proposed that the formed radical species would react with $S_2O_3^{2-}$ and result in the production of $S_4O_6^{2-}$ through reactions 9 and 10. For a more detailed description of the proposed reaction chain and termination, see Littlejohn et al.[11]

$$R^• + S_2O_3^{2-} \rightarrow R + S_2O_3^{•-} \tag{9}$$

$$S_2O_3^{•-} + S_2O_3^{•-} \rightarrow S_4O_6^{2-} \tag{10}$$
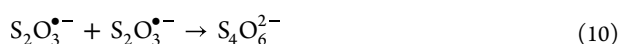
The motivation for research on sulfite oxidation has with time shifted from atmospheric chemistry motivated by the high emissions of SO_2 to WFGD systems employed to control SO_2 emissions and to combined removal systems of NO_x and SO_x. These systems have complex reaction patterns, and the previously applied analysis methods require ex situ measurements, titration, and ion chromatography, which have delivered results that vary by several orders of magnitude. Beilke, Lamb, and Müller[16] studied the uncatalyzed SO_2 oxidation in a closed environment to investigate rate-determining steps in the formation of atmospheric sulfate. Results indicate a first-order reaction in regard to sulfite concentration and a zero-order reaction in regard to oxygen for a pH between 3 and 6. Only SO_2 and SO_4^{2-} were measured, and S(IV) oxidation was assumed to be the rate-limiting step. SO_3^{2-} was assumed to be the reacting species of S(IV), which was supported by a $[H^+]^{-2}$ trend. They

observed no significant dependence on temperature in the interval between 5 and 25 °C. Larson, Horike, and Harrison[17] concur that the uncatalyzed oxidation of SO_2 by O_2 was first order in SO_3^{2-} but expressed the reaction in terms of additional H^+ dependencies of half order in the pH interval between 4 and 12. Unlike the previous study, they did observe a slight temperature dependence in the interval 5−25 °C. Connick et al.[18] continued the study with a focus on the oxidation of bisulfite (pH 4) relevant to flue gas desulfurization (FGD) and atmospheric chemistry, where oxygen concentration and added NaOH was used to determine the reaction path and rate. They suggest that the reaction takes place via HSO_5^- formed from SO_3^{2-}. An expression was formulated for O_2 consumption as second order in HSO_3^- and H^+ and zero order in O_2. Mo et al.[19] investigated the sulfite oxidation rate by oxygen and the inhibiting effect on the oxidation by thiosulfate in a thermostatic reactor with continuous airflow. Continuous pH measurements and titration of the resulting liquid were used as a basis for analysis. They noted a decrease in oxidation rate from pH 6 to pH 3 and almost no effect of pH in the interval 7 to 8. The conclusion was the same as that in the previously mentioned studies where the low activity of HSO_3^- would decrease oxidation rate, and at a certain concentration of SO_3^{2-} the reaction was no longer limited by SO_3^{2-} concentration. The effect of $S_2O_3^{2-}$ as an inhibitor for the uncatalyzed oxidation of S(IV) was observed.

The research on S(IV) oxidation in the presence of NO_2 has been performed in parallel to oxidation by O_2 first due to the presence of NO_2 in the atmosphere and later coupled to flue gas treatment. NO_2 has, as mentioned, a large effect on S(IV) oxidation in the presence of O_2, and the reaction is difficult to study as different approaches have been used and different rates have been proposed. Littlejohn, Wang, and Chang[11] and Rochelle & co-workers[12,15] have performed several studies on sulfite and sulfide oxidation where the influence of NO_2 absorption was investigated. Gas analysis of NO_x was used for the determination of reaction rate, and the solution was analyzed with ion chromatography.

In this study, a similar setup to that used by Huang et al.[20] is used to provide additional information on the reaction of sulfite oxidation. In contrast to earlier studies, an online analysis method in Raman spectroscopy is used. The important advantage of this analysis method is that all reaction products will be possible to identify continuously, which is important in a complex system where both nitrogen and sulfur are present and reaction products include a great variety of species.[21] The advantages of Raman spectroscopy also include that it is a quick, accurate, and nondestructive method that is seeing increased usage and rapid scientific development.[22,23] This study aims to assess the suitability of Raman spectroscopy for liquid-phase analysis in a combined SO_x−NO_x removal system and thereafter investigate the rate of sulfite oxidation while bubbling O_2 through a bubble flask and to compare that rate when NO_2 is present in the gas phase and thiosulfate is present in the liquid phase. The hypothesis is that NO_2 will increase the oxidation rate of sulfite and that thiosulfate will lower the oxidation rate of sulfite, as has been seen in our research and in a study by Schmid et al.[24] The setup is not suitable to provide exact reaction rates, and the rates derived are used for comparison with the vast body of literature present.

Table 1. Summary of Continuous Experiments[a]

Investigation	SO_3^{2-} (mol/kg$_{H2O}$)	HSO_3^{-} (mol/kg$_{H2O}$)	SO_4^{2-} (mol/kg$_{H2O}$)	$S_2O_3^{2-}$ (mol/kg$_{H2O}$)	NO_2^{-} (mol/kg$_{H2O}$)	CO_3^{2-} (mol/kg$_{H2O}$)	NO_2 (ppm)	O_2 (%)
1	0.02	0.02						3
2				0.04				3
3	0.02	0.02		0.04				3
4	0.02	0.02					95	3
5				0.04			95	3
6	0.02	0.02		0.04			95	3
7	0.02	0.02	0.10	0.04	0.02	0.01	95	3

[a]Concentrations correspond to the amount of salt added before equilibrium is reached.

2. MATERIALS AND METHODS

2.1. PLSR Model Preparation for Raman Spectrometer. Chemicals used in this work were sodium salts of sulfite (≥98%), bisulfite (99%), sulfate (≥99%), thiosulfate (≥99%), nitrite (≥99%), nitrate (≥99%), bicarbonate (≥99%), and carbonate (≥99%), all supplied by Sigma-Aldrich. In order to prepare the partial least-squares regression (PLS-R) models, known amount of these chemicals was mixed with known amount of Milli-Q water (resistivity 18.2 MΩ·cm). The methodology used in this study is a multivariate spectroscopic data evaluation approach in which Raman spectra of the seven species as mentioned earlier were carefully calibrated and validated. The procedure is explained below.

2.1.1. Sample Preparation for PLS-R Model Calibration and Validation. For each species studied in this work, a stock solution with a known amount of chemical components in Milli-Q water was prepared. A continuous set of samples with varying species concentrations was then made by diluting the stock with different weights of Milli-Q water in 10 mL sample vials. Typically, 40 samples are prepared for each species: one set of solutions was prepared for PLS-R model calibration, and a second independent set was used for validation. The upper concentration for species studied in this work was determined to include the relevant species concentrations for a combined SO_2 and NO_2 industrial flue gas cleaning system based on experiments and simulations.[25,26] The samples were then analyzed using a Raman spectrometer as soon as they were prepared.

2.1.2. Raman Measurement. In this study, a RXN2 Raman spectrometer fitted with a Kaiser Raman short-focus immersion probe was used. Specifications of the spectrometer and the immersion probe are summarized in Table S1, Supporting Information. The instrument can be operated with a maximum laser power of 400 mW. In this study, the laser power was kept at its highest value of 400 mW to minimize exposure time because low laser power was shown to be insensitive to sulfite peaks. The signal-to-noise (S/N) ratio of the Raman measurements was optimized by changing the exposure time and number of scans. In this work, the optimized S/N ratio was obtained when the exposure time was 90 s with three scans.

Before starting a Raman measurement, the short-focus immersion optic was attached to the fiber optic probe head, and the probe area which would be in contact with the sample was cleaned with ethanol. The immersion probe was then positioned vertically using a stand, with the optical window facing downward. During measurement, it was ensured that the probe was immersed in the sample and the tip of the optic was positioned in the center of the glass vial. The sample and probe optic were protected from external light sources (such as fluorescent light) using aluminum foil. The Raman spectrum was collected using a software called iC Raman (Kaiser Instruments). Before collecting the next spectrum, the Raman probe was cleaned with Milli-Q water and ethanol and wiped to avoid cross-contamination between samples.

2.1.3. Preprocessing of Raman Spectra and PLS-R Modeling. The Raman spectra obtained were exported to Matlab2018a (MathWorks Inc.) and PLS Toolbox 8.6.2 (eigenvector Research Inc.) software for data processing. Measurements were performed in diluted solutions, and in most cases, concentrations of species were very low, making result interpretation a challenge without a suitable preprocessing technique. In this work, the preprocessing method using Whittaker filter ($\lambda = 1$, $\rho = 0.001$) gives satisfactory baseline correction. These preprocessed spectra are then subjected to PLS-R. In all cases, normalization against an instrument peak was also applied. For raw and preprocessed spectra, see Figure S1, Supporting Information.

2.2. Sulfite Oxidation Experiments. Gases with known concentrations of NO_2 and/or O_2 in N_2 are led through a bubbling flask with a prepared batch solution of different salts. Each sample was prepared by weighing each salt and mixing it in a known amount of degassed Milli-Q water in an Erlenmeyer bottle. The sample was then sealed and stirred with a magnetic stirrer before it was weighed again to ensure correct preparation. The gases, 1% NO_2 in N_2, N_2, and O_2, were supplied by Linde gas. The Bronkhorst MFCs were calibrated for 0−0.1 NL/min (O_2), 0−0.019 NL/min (NO_2/N_2), and 0−5 NL/min (N_2). The gases were either led directly to the gas analyzer or through the bubble flask. Before each experiment, the setup was flushed with N_2 to evacuate O_2. The only O_2 present in the system before experiment initiation was that present in the bubble flask. The bubble flask was equipped with an aeration head, the Raman probe, and a pH electrode. Temperature and chemical composition were measured continuously. The pH electrode was connected to a Metrohm 905 Titrando, which was programmed to maintain pH at 7 for the samples by the addition of 0.1 M NaOH. The initial sample pH target of 7 is reached by the addition of an equimolar distribution of Na_2SO_3/ NaHSO₃. The pH control during experiments was, however, unsuccessful during several experiments, with a resulting pH > 9 as too much NaOH was added. The gas analyzer (Testo 350, from Nordtec) measured the concentration of SO_2, O_2, NO, and NO_2 by electrochemical sensors on the basis of selectivity potentiometry. The amount of absorbed NO_2 was estimated by subtracting the measured exit concentration of NO_2 from the amount injected, which was quantified by a continuous log of supplied mV to the MFC. For a figure of the experimental setup, see Figure S2, Supporting Information.

The experimental matrix is specified in Table 1. The experiments were divided into seven sets, denoted "Inves-

Table 2. Characteristic Vibrational Modes for all Chemical Species Observed and Published in Literature[a]

species	observed (cm^{-1})	published (cm^{-1})	refs
$SO_{4(aq)}^{2-}$	449, 613, 981*	449, 613, 981, 1111, 1125	28,29
$SO_{3(aq)}^{2-}$	474, 619, 965*	469, 620, 896, 933, 967	30
$HSO_{3(aq)}^{-}$	1022*, 1052*	235, 655, 730, 1052, 1023, 1052, 2350	31
$NO_{3(aq)}^{-}$	1048*, 1354	676, 713, 717, 719, 743, 770, 823, 830, 1045, 1048, 1050, 1052, 1075, 1342, 1358, 1384, 1413, 1450	32,33
$NO_{2(aq)}^{-}$	816*, 1329*	1323, 2640	34
$CO_{3(aq)}^{2-}$	1067*	680, 1065, 1380, 1436	35
$S_2O_{3(aq)}^{2-}$	336, 448*, 535, 668, 997*	336, 448, 535, 668, 997, 1122	36

[a]The observed peaks which were used for analysis are marked with an asterisk.

Table 3. Rate of Formation of Selected Species and NO$_2$ Absorption Rate from Gas to Liquid During the Continuous Experiments

Investigation	$\dfrac{d[S(IV)]}{dt}\left(\dfrac{mmol}{kg_{H2O}\cdot min}\right)$	$\dfrac{d[SO_4^{2-}]}{dt}\left(\dfrac{mmol}{kg_{H2O}\cdot min}\right)$	$\dfrac{d[S_2O_3^{2-}]}{dt}\left(\dfrac{mmol}{kg_{H2O}\cdot min}\right)$	NO$_2$ absorption rate $\left(\dfrac{mmol}{kg_{H2O}\,min}\right)$	$[S(IV)]_{ox}/[NO_2]_{abs}$ (mmol/mmol)
1	−0.07	0.06			
2	0.01	−0.00	0.02		
3	−0.00	0.00	0.00		
4	−0.84	0.54		0.028	−30.6
5	0.00	0.00	−0.00	0.020	0
6	−0.06	0.12	−0.04	0.030	−2.35
7	0.01	0.06	−0.04	0.032	0.88

tigations". Each investigation had a specific aim. Investigation 1 aimed to study the rate of sulfite oxidation from O$_2$ gas at a partial pressure of 3 kPa, 3%. Investigation 2 replicated Investigation 1 but with Na$_2$S$_2$O$_3$ instead of Na$_2$SO$_3$ to investigate the oxidation rate of thiosulfate by O$_2$. Investigation 3 aimed to establish the effect of thiosulfate on sulfite oxidation by O$_2$. Investigations 4 to 6 corresponded to Investigations 1 to 3 but with NO$_2$ present in the gas phase to establish the influence of NO$_2$ on the reaction chemistry. Investigation 7 had a liquid composition similar to what was expected for a combined NO$_x$ and SO$_x$ absorption system. The aim of Investigation 7 was to evaluate the suitability of the measurement technique used for process control in a combined NO$_x$ and SO$_x$ absorption system.

3. RESULTS AND DISCUSSION

3.1. Spectra Preprocessing and Peaks Assignment. For spectrum preprocessing, the Whittaker algorithm[27] was employed to reduce baseline noise and thereby provide an improved spectrum for further analytical purposes. Table 2 shows a list of Raman vibrational bands that were observed in this study in comparison to available data from the literature. Measurements in this work were performed on diluted and low-concentration species, and some signals were not significant. For example, the antisymmetric stretching SO$_4^{2-}$ signal at 1111 cm^{-1} observed by Irish, D., and Chen, H., was not visible in this work. Instead, the PLS-R model for sulfate is based on the peak at 981 cm^{-1}, which was distinct and, after preprocessing, clearly separated from other peaks. Of the seven chemical species studied in this work, at least one Raman peak could be used for PLS-R modeling, and the peak with the lowest associated error was used for analysis. The peaks used are marked with an asterisk in Table 2.

It is known that sulfite, bisulfite, and to some extent thiosulfate are oxidized to sulfate in the presence of air or O$_2$. During measurements, small increment to the sulfate peak at 981 cm^{-1} could be seen as the concentration of sulfite increased. This oxidation, albeit small, will affect the accuracy of the PLS-R models. Therefore, in this work, initial concentrations of sulfite,

bisulfite, and thiosulfate were corrected to compensate the possible oxidation.

Based on the preprocessed Raman spectra, PLS-R models for sulfate, sulfite, bisulfite, thiosulfate, nitrite, nitrate, and carbonate were constructed. The final and optimized PLS-R models for the species studied in this work show low error of prediction (RMSEP) values, suggesting good reliability of these models: the highest RMSEP value is 0.00627 for CO$_3^{2-}$, while the lowest RMSEP value is 0.00092 for SO$_4^{2-}$. For a complete summary of the individual calibrations, see Figure S3 and Table S2, Supporting Information.

3.2. Continuous Liquid Composition Analysis Experiments. Table 3 compiles the rate of formation for the species of interest from each Investigation. Initial concentrations are given in Table 1. In addition, Table 3 presents the NO$_2$ absorption rate—estimated by comparing gas analyzer outlet concentrations of NO$_x$ with MFC-voltage for the NO$_2$ inlet—as well as the ratio of oxidized moles of S(IV) to the NO$_2$ absorption rate. S(IV) includes both SO$_3^{2-}$ and HSO$_3^{-}$. When comparing the result of Investigations 1 and 4, it is obvious that NO$_2$ absorption increases the oxidation of S(IV), as the S(IV) oxidation rate is 10 times higher in the presence of NO$_2$ than when only O$_2$ is present. This is supported by the formation of a sulfite radical in reaction 8. Investigations 3 and 6 show that S$_2$O$_3^{2-}$ is efficient at inhibiting S(IV) oxidation by eliminating the radical chain reaction as described by reactions 9 and 10, as there is no oxidation taking place without NO$_2$ presence and the oxidation of S(IV) is reduced by ∼75% when NO$_2$ is present. The bubble flask has a baseline of absorption of NO$_x$ at ∼6% and NO$_2$ at ∼17%.

3.2.1. Sulfite Oxidation without NO$_2$ Presence. Figure 2 shows the concentration profiles for Investigation 1. The initial flushing with N$_2$ is finished and O$_2$ injected 800 s after the log started. The initial concentrations of HSO$_3^{-}$ (0.02 mol/kg$_{H_2O}$) and SO$_3^{2-}$ (0.02 mol/kg$_{H_2O}$) are stable at the start of the experiment. The total amount of sulfur analyzed remains close to the starting concentration of 0.04 mol/kg$_{H_2O}$. The distribution
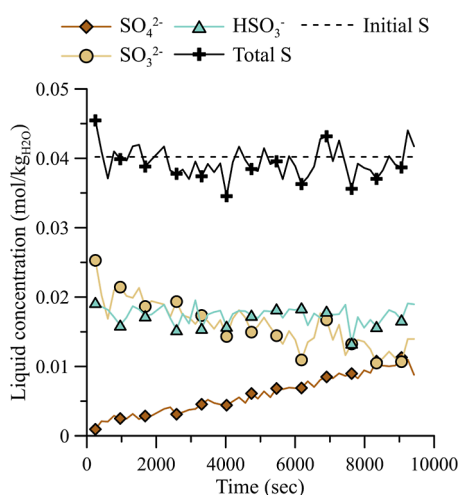
Figure 2. Concentration profile for Investigation 1: 20 °C, pH ∼ 7, and 3% O_2. Total S is the total molar concentration of sulfur species analyzed by Raman spectroscopy. Initial S is the by weight estimated amount of moles of sulfur added to the sample.

between HSO_3^- and SO_3^{2-} changes with the pH, following the equilibrium from a pH of 7.1 at the start of the experiment to a pH of 6.7 at the end of the experiment (see Figure S4, Supporting Information). The rate of SO_4^{2-} formation observed can be compared to the rate expression obtained by Zhang and Millero[37] with second-order dependence on sulfite concentration and 0.5 order dependence on O_2 concentration. For O_2 concentration profile and Raman spectra profile, see Figures S5 and S6, Supporting Information.

Figure 3 shows the concentration profile for Investigation 2. The initial flushing with N_2 is finished and O_2 injection started at
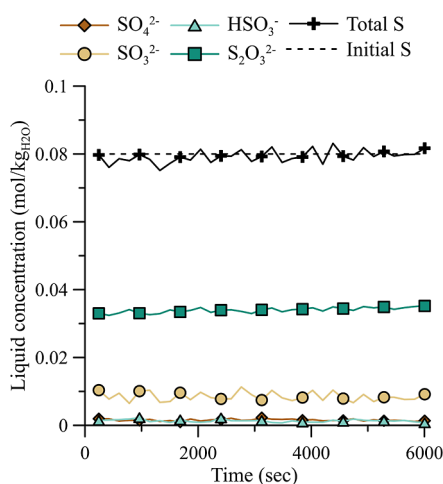

Figure 3. Concentration profile for Investigation 2, 20 °C, pH ∼ 7.1, and 3% O_2. Total S is the total molar concentration of sulfur species analyzed by Raman spectroscopy. Initial S is the by weight estimated amount of moles of sulfur added to the sample.

1100 s. SO_3^{2-} and HSO_3^- are detected from the start of the measurements, formed from the introduced $S_2O_3^{2-}$ (0.04 mol/kg_{H_2O}). The solution is bubbled with 3% O_2 in N_2. There is no clear oxidation of $S_2O_3^{2-}$ taking place by O_2, which is in agreement with the previous work.[38] The pH increased from 7.1 at the start to 7.7 when the log ended (see Figure S7, Supporting

Information). For O_2 concentration profile and Raman spectra profile, see Figures S8 and S9, Supporting Information.

Figure 4 shows the concentration profile for Investigation 3. The initial flushing with N_2 is finished and O_2 injection started
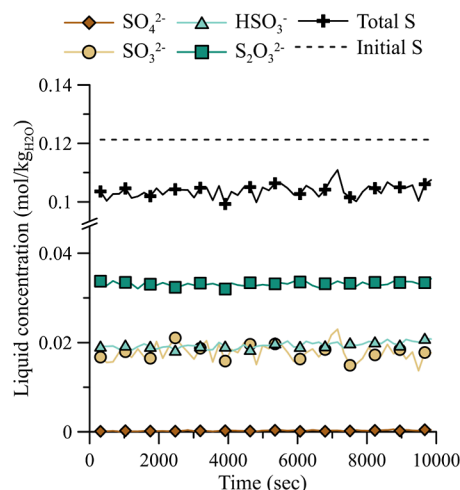

Figure 4. Concentration profile for Investigation 3, 20 °C, pH ∼ 7.0, and 3% O_2. Total S is the total molar concentration of sulfur species analyzed by Raman spectroscopy. Initial S is the by weight estimated amount of moles of sulfur added to the sample.

1000 s after the log started. The initial concentrations of HSO_3^- (0.02 mol/kg_{H_2O}) and SO_3^{2-} (0.02 mol/kg_{H_2O}) remain stable throughout the experiment. The added amount of $S_2O_3^{2-}$ (0.04 mol/kg_{H_2O}) is directly reduced to 0.03 mol/kg_{H_2O} and then constant throughout the experiment. It is evident that $S_2O_3^{2-}$ inhibits the oxidation of SO_3^{2-} by O_2 and the formation of SO_4^{2-} when comparing the result with Investigation 1 in Figure 2. The pH remains constant at 7 throughout the experiment, see Figure S10, Supporting Information. For O_2 concentration profile and Raman spectra profile, see Figures S11 and S12, Supporting Information.

3.2.2. Sulfite Oxidation with NO₂ Presence. Figure 5 shows the concentration profile for Investigation 4. The initial flushing with N_2 is finished and O_2 and NO_2 injection started 1400 s after the log started. The total S concentration initially deviated from the starting concentration. The deviation corresponds to a low reading in SO_3^{2-} and HSO_3^- that could be attributed to noise in the Raman peak. SO_4^{2-} is rapidly increasing after 1400 s, and the rate of formation gradually decreases until reaching a stable concentration at 6000 s. The pH remains around 7 until the SO_3^{2-} and HSO_3^- concentrations are diminished at around 4000 s into the experiment. It then overshoots the addition of NaOH, and pH increases to 11 (see Figure S13, Supporting Information).

The combined rate of consumption of S(IV) in the initial time period 1000−3000 s is 0.85 mmol·$kg_{H_2O}^{-1}$ min^{-1}. The rate is comparable to, but lower than, the rate observed by Schmidt et al. of 2.5 mmol·$kg_{H_2O}^{-1}$ min^{-1}.[39] There is no nitrogen salt in the prepared sample, and according to the mass balance based on gas analysis, the nitrogen concentration in the liquid should be around 0.005 mol/kg_{H_2O} at the end of the experiments. The absorbed concentration is below the detection limit for NO_2^- and NO_3^-.
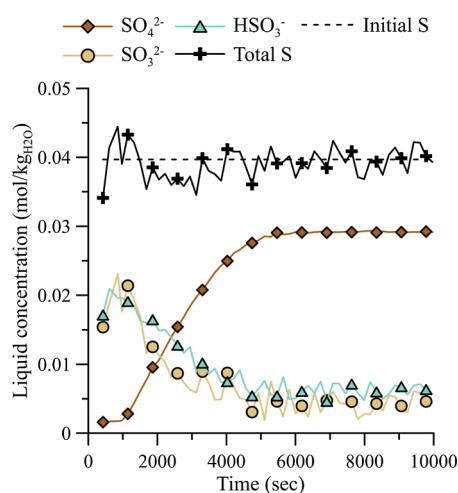
Figure 5. Concentration profile during Investigation 4: 20 °C, pH ∼ 7.1, 95 ppm NO_2, and 3% O_2. Total S is the total molar concentration of sulfur species analyzed by Raman spectroscopy. Initial S is the by weight estimated amount of moles of sulfur added to the sample. The initial flushing with N_2 is finished at 1400 s on the y-axis. The pH is constant at 7 until 4000 s where it increases to 11.

When comparing the S(IV) oxidation rate between Investigations 4 and 1, it is clear that NO_2 absorption initiates a radical chain reaction where S(IV) is oxidized to S(VI) as shown by reaction 8. The molar ratio between oxidized S(IV) and absorbed NO_2 is ∼31, which can be compared to the stoichiometry of 1 for the global reaction of NO_2 absorption in SO_3^{2-}. See Figure S14, Supporting Information, for a gas concentration profile of NO_x and O_2 during the investigation and Figure S15 for a Raman spectra profile.

Figure 6 shows the concentration profile for Investigation 5 with an initial concentration of $S_2O_3^{2-}$ (0.04 mol/kg$_{H_2O}$) and bubbled with 3% O_2 and 95 ppm NO_2 in N_2. The initial flushing with N_2 is finished and O_2 injection started at 1400 s after the log started. The concentration profile shows similar trends to
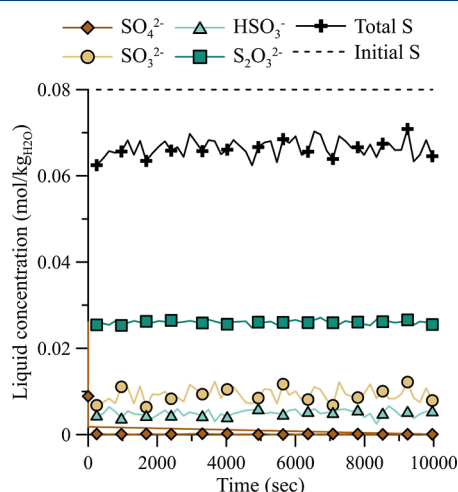

Figure 6. Concentration profile during Investigation 5, 20 °C, pH ∼ 5.5, 95 ppm NO_2, and 3% O_2. Total S is the total molar concentration of sulfur species analyzed by Raman spectroscopy. Initial S is the by weight estimated amount of moles of sulfur added to the sample. The initial flushing with N_2 is finished at 900 s on the y-axis. The pH starts at 7, increases to 7.5 within 1000 s, and then decreases to 5.5 at 5000 s, where it remains stable for the rest of the experiment.

Investigation 2. Total S concentration remains slightly below that of the weight estimated in sample preparation throughout the experiment. The SO_3^{2-} formed together with $S_2O_3^{2-}$ absorbs part of the NO_2 without clear consumption of the species. The pH increases from 7 to 7.5 initially and then decreases with the start of O_2/NO_2 injection until around 4000 s, when it stabilizes at pH 5.5 (see Figure S16, Supporting Information). For O_2 concentration profile and Raman spectra profile, see Figures S17 and S18, Supporting Information.
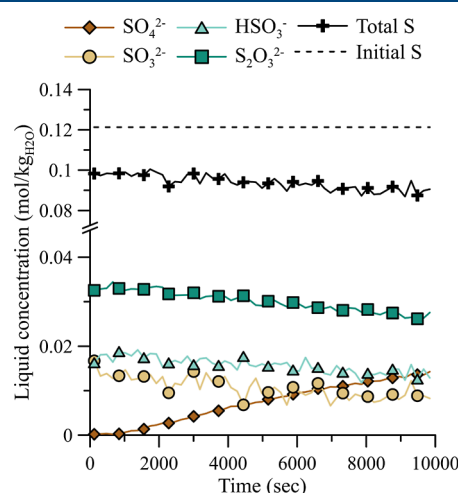

Figure 7. Concentration profile during Investigation 6, 20 °C, pH ∼ 6.9, 95 ppm NO_2, and 3% O_2. Total S is the total molar concentration of sulfur species analyzed by Raman spectroscopy. Initial S is the by weight estimated amount of moles of sulfur added to the sample. The initial flushing with N_2 is finished at 1800 s on the y-axis.

Figure 7 shows the concentration profile for Investigation 6 with an initial concentration of HSO_3^- (0.02 mol/kg$_{H_2O}$), SO_3^{2-} (0.02 mol/kg$_{H_2O}$), and $S_2O_3^{2-}$ (0.04 mol/kg$_{H_2O}$) and bubbled with 95 ppm NO_2, 3% O_2 in N_2. The initial flushing with N_2 is finished and O_2 and NO_2 injection started 1800 s after the log started. Initial concentration of total S is almost 20% off primarily due to the initial concentration of $S_2O_3^{2-}$ (0.032 instead of 0.04). Both SO_3^{2-} and HSO_3^- are decreasing with time, and the SO_3^{2-} concentration remains below that of HSO_3^- throughout the experiment, following the pH. The combined rate of consumption of S(IV) after initial flushing is 0.07 mmol·kg$_{H_2O}^{-1}$ min^{-1}. The rate is comparable to but lower than that observed by Schmidt et al. of 0.23 mmol·kg$_{H_2O}^{-1}$ min^{-1}.[39]

The total S concentration is diminishing with time, and an unidentified molecule is likely formed. In the Raman spectra, an unidentified peak at 259 cm^{-1} is steadily increasing with time (see Figure S21, Supporting Information). A previously documented species formed from NO_2 absorption with $S_2O_3^{2-}$ is $S_2O_6^{2-}$; however, no Raman peaks have been reported for $S_2O_6^{2-}$ at 259 cm^{-1} in the reviewed literature. There are also studies that identify a number of nitrososulfonates (nitrogen-sulfur compounds) which can form in the bulk solution of a NO_2−S(IV) mixture; the formation is however more prevalent in acidic solutions. The only reference[40] to a peak in nearby regions for a species that has been documented as a product in NO_2 absorption with $S_2O_3^{2-}$ is a peak at 260 cm^{-1} of $S_4O_6^{2-}$, tetrathionate, which is the product of reaction 10. The pH starts

at 6.9 and decreases to 6.7 at the end of the experiment (see Figure S19, Supporting Information). For O_2 concentration profile and Raman spectra profile, see Figures S20 and S21, Supporting Information.
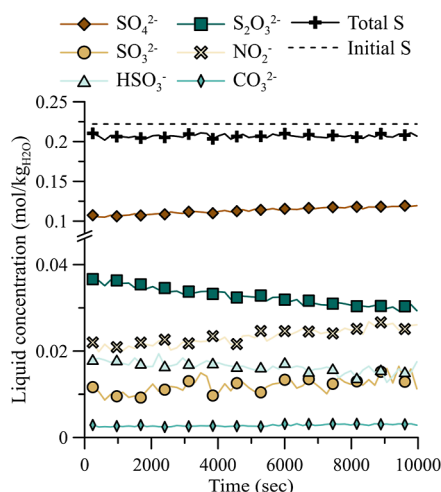

Figure 8. Concentration profile during Investigation 7, 20 °C, pH increasing from 7.1 to 8.5, 95 ppm NO_2, and 3% O_2. Total S is the total molar concentration of sulfur species analyzed by Raman spectroscopy. Initial S is the by weight estimated amount of moles of sulfur added to the sample.

Figure 8 shows the concentration profile for Investigation 7 with initial concentrations of HSO_3^- (0.02 mol/kg_{H_2O}), SO_3^{2-} (0.02 mol/kg_{H_2O}), $S_2O_3^{2-}$ (0.04 mol/kg_{H_2O}), SO_4^{2-} (0.1 mol/kg_{H_2O}), NO_2^- (0.02 mol/kg_{H_2O}), and HCO_3^- (0.01 mol/kg_{H_2O}) and bubbled with 95 ppm NO_2, 3% O_2 in N_2. The initial flushing with N_2 is finished and O_2 injection started 1100 s after the log started. Initial concentration of total S is around 10% off primarily due to the initial concentration of $S_2O_3^{2-}$ (0.036 instead of 0.04). The total S concentration is constant throughout the experiment, unlike that in Investigation 6. When comparing the results in Figure 8 of Investigation 7 with those in Investigation 6 and Figure 7, it is evident that the addition of either CO_3^{2-} or NO_2^- limits the S(IV) oxidation. When there is no $S_2O_3^{2-}$ present, SO_3^{2-} oxidation should increase with increasing concentrations of NO_2^- according to previous studies, something which is not observed in this experiment.[20,41] The observed difference could also be due to the alkaline pH in this experiment compared to the acidic used in the mentioned references where NO_2^- is considerably less stable. Only 0.01 mmol·$kg_{H_2O}^{-1}$ min^{-1} of HSO_3^- is consumed, but the total S(IV) concentration is more or less constant since SO_3^{2-} is increasing with 0.02 mmol·$kg_{H_2O}^{-1}$ min^{-1}. The analysis result of decreased S(IV) oxidation is supported by the lowered rate of formation of SO_4^{2-} which is only half of that in Investigation 6. The rate of consumption of $S_2O_3^{2-}$ is the same in both Investigations 6 and 7. The results for NO_2^- are included here since the high concentration from initial sample preparation makes quantification possible. There is a clear trend of increasing NO_2^- concentration over time from ~21 to ~26 mM, which corresponds to the absorbed amount of NO_2 estimated from the analysis of the gas to 4.7 mM.

Similar to Investigation 6, there is an unidentified peak at 259 cm^{-1} present, but only at half the intensity (see Figure S24, Supporting Information). The pH increases from 7 to 8.2 in the first 4500 s and then increases rapidly to pH 10 (see Figure S22, Supporting Information). For O_2 concentration profile and Raman spectra profile, see Figures S23 and S24, Supporting Information.

4. SUITABILITY AND APPLICATION OF RAMAN SPECTROSCOPY FOR ONLINE MEASUREMENTS IN A COMBINED SO_X−NO_X REMOVAL SYSTEM

The results obtained in this study show that Raman-spectroscopy can speciate and quantify SO_3^{2-}, HSO_3^-, SO_4^-, and $S_2O_3^{2-}$ even in mixtures with NO_2^-, NO_3^-, and CO_3^{2-}. The sharp peak at 981 cm^{-1} gives a clear signal for SO_4^{2-} even at a concentration of 3 mM. The broad peak at 965 cm^{-1} is suitable for SO_3^{2-} quantification; however, the signal is less stable, and concentrations should be >10 mM to avoid interference with background noise. The same is true for HSO_3^- which has broad peaks at 1022 and 1052 cm^{-1}. $S_2O_3^{2-}$ is identified through a sharp peak at 997 and 448 cm^{-1} which gives a clear signal in the tested concentration range 20−40 mM.

Quantification of NO_2^- and NO_3^- is difficult in the present system with the chosen method. The low concentrations present in Investigations 1−6 are not possible to quantify. In Investigation 7 where NO_2^- is present at a higher concentration of 20 mM, it is quantifiable with some degree of uncertainty. However, the fact that the nitrogen balance is close to complete when accounting for the absorbed NO_2 indicates the success of the measurement.

The limit of detection for some species could be an issue for the u-e of Raman spectroscopy as a method for on line liquid analysis in a NO_x−SO_x removal system. The species include SO_3^{2-}, HSO_3^-, and NO_3^-. In this study, the concentrations of SO_3^{2-} and HSO_3^- are required to be ~20 mM each, together with ~30 mM $S_2O_3^{2-}$ to reach 80% NO_2 absorption. This is above the 10 mM minimum recommended limit of detection in this study. However, in our previous studies[25] where absorption units that are designed to maximize NO_2 absorption have been used, 80% NO_2 absorption was reached at only 1 g/L of Na_2SO_3, corresponding to ~6 mM. In these studies, no $S_2O_3^{2-}$ was added to the liquid, and it was of interest to minimize the S(IV) added due to the rapid oxidation to SO_4^{2-}, which means higher Na_2SO_3 consumption and therefore an increased cost of operation. The results in Figure 8 indicate that $S_2O_3^{2-}$ is so efficient at limiting S(IV) oxidation that higher concentrations of S(IV) should be mainly beneficial due to increased NO_2 absorption. It is therefore likely that a NO_x−SO_x scrubber unit will be operating above 10 mM of SO_3^{2-} if $S_2O_3^{2-}$ is added. This result is in agreement with the findings of Sapkota et al.[12] NO_3^- is only present in concentrations below 10 mM and should therefore with the present model not be quantifiable by Raman spectroscopy, as it is not one of the main products in the reaction chain. If a strong oxidizer is present in the liquid phase, such as when O_3 is used for the oxidation and absorption of NO_2, then NO_3^- will form from NO_2^-, resulting in higher concentrations, possibly above detection limits where usage of Raman spectroscopy could be suitable.

Raman spectroscopy is potentially a good analysis technique that in combination with standard gas analysis can be used for process control in a combined SO_2 and NO_2 flue gas cleaning system with large changes in concentration- and flow-profiles over time. The absorption rates of NO_2 and SO_2 would then

continuously be monitored through gas analysis while the concentrations of salts are quantified by the Raman instrument. This will enable exact control of liquid bleed amounts to minimize the loss of chemicals and addition of water while at the same time showing a precise need for addition of Na_2SO_3 and $Na_2S_2O_3$ needed for NO_2 absorption to maintain balance. For flue gas sources with stable concentration- and flow-profiles, simpler and less costly instruments, such as conductivity or redox meters, can be used after an initial testing period with Raman spectroscopy that characterize the scrubber and connect it to conductivity and / or redox potential.

5. FUTURE WORK

This initial study shows promising results both in interpreting the reaction mechanism of S(IV) oxidation with NO_2 absorption and monitoring the liquid phase composition. There are however several points that need further investigation. The unidentified peaks at 259, 665, 734, 1052, and 1384 cm^{-1} need to be further studied to enable speciation. If possible, new peaks for NO_2^- and NO_3^- should be identified and used for quantification; in the case of NO_2^-, much higher concentrations can be used since concentrations in an actual flue gas cleaning system preferably are as close to the precipitation limit as the system can handle.

After the questions in this study have been answered, more complex liquids can be studied. In a combined NO_2 and SO_2 flue gas cleaning system, a wide number of other impurities, depending on the flue gas source, will be present. Most of these will only be present in limited concentrations, but their spectra could still disrupt the Raman peaks used in this study. Some of the possible impurities like iron, manganese, and copper are also reported in the literature to have a catalytic effect on S(IV) oxidation,[15] which is something that could be investigated with the method used in this study.

6. CONCLUSIONS

Seven PLS-R models for SO_3^{2-}, HSO_3^-, $S_2O_3^{2-}$, SO_4^{2-}, NO_2^-, NO_3^-, and CO_3^{2-} were developed using Raman spectroscopy. The models are applied to evaluate sulfite and bisulfite oxidation in a bubbling flask. Two oxidant compositions are investigated: O_2 at 3% and O_2 at 3% with NO_2 at 95 ppm. The oxidation of sulfite and bisulfite is also investigated with the addition of a free radical scavenger in $Na_2S_2O_3$. The key findings are summarized below.

1. Raman Vibrational bands of SO_3^{2-}, HSO_3^-, $S_2O_3^{2-}$, SO_4^{2-}, NO_2^-, CO_3^{2-}, and CO_3^{2-} are successfully identified and possible to separate from each other even in mixtures. Raman spectroscopy is a suitable method for liquid analysis of a combined NO_x/SO_x removal system.

2. S(IV) is oxidized at a rate of ~0.07 mmol/$(kg_{H_2O}\cdot min)$ when the bubble flask is fed with 3% O_2 in N_2. Total sulfur concentration remains constant, indicating that no other species than SO_4^{2-} is formed. When $S_2O_3^{2-}$ is added to the liquid, no S(IV) is oxidized by O_2.

3. With NO_2 present in the gas phase, the S(IV) oxidation increases to 0.84 mmol/$(kg_{H_2O}\cdot min)$. The total S(IV) oxidation is increased by a factor of 10 compared to oxidation by the gas without NO_2 (i.e., only containing O_2). The ratio between absorbed NO_2 and oxidized S(IV) is ~31, confirming the reaction scheme of S(IV) oxidation with a radical chain.

4. Addition of $S_2O_3^{2-}$ to the liquid inhibits or even eliminates the S(IV) oxidation even though NO_2 is absorbed. With a concentration of 35 mM $S_2O_3^{2-}$ and 20 mM SO_3^{2-} and HSO_3^-, 80% of the incoming NO_2 is absorbed, and no S(IV) oxidation takes place while $S_2O_3^{2-}$ is consumed at a rate of 0.04 mmol/$(kg_{H_2O}\cdot min)$ with a NO_2 absorption rate of 0.032 mmol/$(kg_{H_2O}\cdot min)$.

■ ASSOCIATED CONTENT

Ⓢ Supporting Information

The Supporting Information is available free of charge at https://pubs.acs.org/doi/10.1021/acs.iecr.3c01015.

Additional information about the spectrometer and additional experimental results, including Raman spectra profiles and gas concentrations (PDF)

■ AUTHOR INFORMATION

Corresponding Author

Jakob Johansson − *Department of Space, Earth and Environment, Chalmers University of Technology, 41296 Gothenburg, Sweden;* ⓞ orcid.org/0000-0001-8011-7783; Phone: +46 31 7725248; Email: jakobjo@chalmers.se

Authors

Jayangi D. Wagaarachchige − *Faculty of Technology, Natural Sciences and Maritime Sciences, University of South-Eastern Norway, 3918 Porsgrunn, Norway;* ⓞ orcid.org/0000-0002-1544-7169

Fredrik Normann − *Department of Space, Earth and Environment, Chalmers University of Technology, 41296 Gothenburg, Sweden*

Zulkifli Idris − *Faculty of Technology, Natural Sciences and Maritime Sciences, University of South-Eastern Norway, 3918 Porsgrunn, Norway*

Eirik R. Haugen − *Faculty of Technology, Natural Sciences and Maritime Sciences, University of South-Eastern Norway, 3918 Porsgrunn, Norway*

Maths Halstensen − *Faculty of Technology, Natural Sciences and Maritime Sciences, University of South-Eastern Norway, 3918 Porsgrunn, Norway*

Wathsala Jinadasa − *Faculty of Technology, Natural Sciences and Maritime Sciences, University of South-Eastern Norway, 3918 Porsgrunn, Norway*

Klaus J. Jens − *Faculty of Technology, Natural Sciences and Maritime Sciences, University of South-Eastern Norway, 3918 Porsgrunn, Norway;* ⓞ orcid.org/0000-0002-9022-5603

Klas Andersson − *Department of Space, Earth and Environment, Chalmers University of Technology, 41296 Gothenburg, Sweden;* ⓞ orcid.org/0000-0001-5968-9082

Complete contact information is available at:
https://pubs.acs.org/10.1021/acs.iecr.3c01015

Notes

The authors declare no competing financial interest.

■ ACKNOWLEDGMENTS

■ REFERENCES

(1) Johansson, J.; Normann, F.; Sarajlic, N.; Andersson, K. Technical-Scale Evaluation of Scrubber-Based, Co-Removal of NO_x and SO_x Species from Flue Gases via Gas-Phase Oxidation. *Ind. Eng. Chem. Res.* **2019**, *58* (48), 21904−21912.

(2) Nash, T. The Effect of Nitrogen Dioxide and of Some Transition Metals on the Oxidation of Dilute Bisulphite Solutions. *Atmos. Environ.* **1979**, *13* (8), 1149−1154.

(3) Beyad, Y.; Burns, R.; Puxty, G.; Maeder, M. A Speciation Study of Sulfur(IV) in Aqueous Solution. *Dalton Trans.* **2014**, *43* (5), 2147−2152.

(4) Siddiqi, M. A.; Krissmann, J.; PetersGerth, P.; Luckas, M.; Lucas, K. Spectrophotometric measurement of the vapour-liquid equilibria of (sulphur dioxide + water). *J. Chem. Thermodyn.* **1996**, *28* (7), 685−700.

(5) Voegele, A. F.; Tautermann, C. S.; Loerting, T.; Hallbrucker, A.; Mayer, E.; Liedl, K. R. About the Stability of Sulfurous Acid (H2SO3) and Its Dimer. *Chem.—Eur. J.* **2002**, *8* (24), 5644−5651.

(6) Rhee, J. S.; Dasgupta, P. K. The Second Dissociation Constant of Sulfur Dioxide-Water. *J. Phys. Chem.* **1985**, *89* (9), 1799−1804.

(7) Schwartz, S. E. Equilibria in the Nitrogen-Oxide Nitrogen Oxyacid-Water System. *Abstr. Pap. Am. Chem. Soc.* **1980**, *180* (Aug), 221-Phys.

(8) Lee, Y. N.; Schwartz, S. E. Reaction-Kinetics of Nitrogen-Dioxide with Liquid Water at Low Partial-Pressure. *J. Phys. Chem.* **1981**, *85* (7), 840−848.

(9) Park, J. Y.; Lee, Y. N. Solubility and Decomposition Kinetics of Nitrous-Acid in Aqueous-Solution. *J. Phys. Chem.* **1988**, *92* (22), 6294−6302.

(10) Clifton, C. L.; Altstein, N.; Huie, R. E. Rate constant for the reaction of nitrogen dioxide with sulfur(IV) over the pH range 5.3-13. *Environ. Sci. Technol.* **1988**, *22* (5), 586−589.

(11) Littlejohn, D.; Wang, Y.; Chang, S. G. Oxidation of Aqueous Sulfite Ion by Nitrogen Dioxide. *Environ. Sci. Technol.* **1993**, *27* (10), 2162−2167.

(12) Sapkota, V. N. A.; Fine, N. A.; Rochelle, G. T. NO2-Catalyzed Sulfite Oxidation. *Ind. Eng. Chem. Res.* **2015**, *54* (17), 4815−4822.

(13) Sun, Y.; Hong, X. W.; Zhu, T. L.; Guo, X. Y.; Xie, D. Y. The Chemical Behaviors of Nitrogen Dioxide Absorption in Sulfite Solution. *Appl. Sci.* **2017**, *7* (4), 377.

(14) Zhuang, Z.; Sun, C.; Zhao, N.; Wang, H.; Wu, Z. Numerical simulation of NO_2 absorption using sodium sulfite in a spray tower. *J. Chem. Technol. Biotechnol.* **2016**, *91* (4), 994−1003.

(15) Shen, C. H.; Rochelle, G. T. Nitrogen Dioxide Absorption and Sulfite Oxidation in Aqueous Sulfite. *Environ. Sci. Technol.* **1998**, *32* (13), 1994−2003.

(16) Beilke, S.; Lamb, D.; Müller, J. On the Uncatalyzed Oxidation of Atmospheric SO2 by Oxygen in Aqueous Systems. *Atmos. Environ.* **1975**, *9* (12), 1083−1090.

(17) Larson, T. V.; Horike, N. R.; Harrison, H. Oxidation of sulfur dioxide by oxygen and ozone in aqueous solution: A kinetic study with significance to atmospheric rate processes. *Atmos. Environ.* **1978**, *12* (8), 1597−1611.

(18) Connick, R. E.; Zhang, Y. X.; Lee, S. Y.; Adamic, R.; Chieng, P. Kinetics and Mechanism of the Oxidation of Hso3- by O-2.1. The Uncatalyzed Reaction. *Inorg. Chem.* **1995**, *34* (18), 4543−4553.

(19) Mo, J. S.; Wu, Z. B.; Cheng, C. J.; Guan, B. H.; Zhao, W. R. Oxidation Inhibition of Sulfite in Dual Alkali Flue Gas Desulfurization System. *J. Environ. Sci.* **2007**, *19* (2), 226−231.

(20) Huang, X.; Ding, J.; Jia, Y.; Zhang, S.; Zhong, Q. Kinetics of Sulfite Oxidation in the Simultaneous Desulfurization and Denitrification of the Oxidation-Absorption Process. *Chem. Eng. Technol.* **2015**, *38* (5), 797−803.

(21) Ajdari, S.; Normann, F.; Andersson, K.; Johnsson, F. Reduced Mechanism for Nitrogen and Sulfur Chemistry in Pressurized Flue Gas Systems. *Ind. Eng. Chem. Res.* **2016**, *55* (19), 5514−5525.

(22) Xu, J.; He, Q.; Xiong, Z.; Yu, Y.; Zhang, S.; Hu, X.; Jiang, L.; Su, S.; Hu, S.; Wang, Y.; Xiang, J. Raman Spectroscopy as a Versatile Tool for Investigating Thermochemical Processing of Coal, Biomass, and Wastes: Recent Advances and Future Perspectives. *Energy Fuels* **2021**, *35* (4), 2870−2913.

(23) Henry, D. G.; Jarvis, I.; Gillmore, G.; Stephenson, M. Raman Spectroscopy as a Tool to Determine the Thermal Maturity of Organic Matter: Application to Sedimentary, Metamorphic and Structural Geology. *Earth Sci. Rev.* **2019**, *198*, 102936.

(24) Schmid, D.; Hupa, M.; Paavola, M.; Vuorinen, I.; Lehikoinen, A.; Karlström, O. Role of Thiosulfate in NO2 Absorption in Aqueous Sulfite Solutions. *Ind. Eng. Chem. Res.* **2023**, *62* (1), 105−110.

(25) Johansson, J.; Heijnesson Hultén, A.; Normann, F.; Andersson, K. Simultaneous Removal of NO_x and SO_x from Flue Gases Using ClO2: Process Scaling and Modeling Simulations. *Ind. Eng. Chem. Res.* **2021**, *60* (4), 1774−1783.

(26) Johansson, J.; Normann, F.; Andersson, K. Techno-Economic Evaluation of Co-Removal of NOx and SOx Species from Flue Gases via Enhanced Oxidation of NO by ClO2-Case Studies of Implementation at a Pulp and Paper Mill, Waste-to-Heat Plant and a Cruise Ship. *Energies* **2021**, *14*, 8512.

(27) Whittaker, E. T. On a New Method of Graduation. *Proc. Edinb. Math. Soc.* **1922**, *41*, 63−75.

(28) Irish, D. E.; Chen, H. Raman Spectral Study of Bisulfate-Sulfate Systems. II. Constitution, Equilibriums, and Ultrafast Proton Transfer in Sulfuric Acid. *J. Phys. Chem.* **1971**, *75* (17), 2672−2681.

(29) Kruus, P.; Hayes, A. C.; Adams, W. A. Determination of Ratios of Sulfate to Bisulfate Ions in Aqueous Solutions by Raman Spectroscopy. *J. Solution Chem.* **1985**, *14* (2), 117−128.

(30) Evans, J. C.; Bernstein, H. J. The Vibrational Spectrum of the Sulphite Ion in Sodium Sulphite. *Can. J. Chem.* **1955**, *33* (7), 1270−1272.

(31) Littlejohn, D.; Walton, S. A.; Chang, S.-G. A Raman Study of the Isomers and Dimer of Hydrogen Sulfite Ion. *Appl. Spectrosc.* **1992**, *46* (5), 848−851.

(32) Waterland, M. R.; Stockwell, D.; Kelley, A. M. Symmetry Breaking Effects in NO3-: Raman Spectra of Nitrate Salts and Ab Initio Resonance Raman Spectra of Nitrate-Water Complexes. *J. Chem. Phys.* **2001**, *114* (14), 6249−6258.

(33) Irish, D. E.; Walrafen, G. E. Raman and Infrared Spectral Studies of Aqueous Calcium Nitrate Solutions. *J. Chem. Phys.* **1967**, *46* (1), 378−384.

(34) Reichenbächer, M.; Popp, J. *Challenges in Molecular Structure Determination*; Springer Science & Business Media, 2012; pp 63−143.

(35) Wen, N.; Brooker, M. H. Ammonium Carbonate, Ammonium Bicarbonate, and Ammonium Carbamate Equilibria: A Raman Study. *J. Phys. Chem.* **1995**, *99* (1), 359−368.

(36) Sun, S.; Cai, T.; Liu, Y.; Wang, J. Experimental and Theoretical Study of the Raman Spectra of Ammonium Thiosulfate Solution. *J. Appl. Spectrosc.* **2015**, *82* (2), 182−187.

(37) Zhang, J.-Z.; Millero, F. J. The Rate of Sulfite Oxidation in Seawater. *Geochim. Cosmochim. Acta* **1991**, *55* (3), 677−685.

(38) Rolia, E.; Chakrabarti, C. L. Kinetics of Decomposition of Tetrathionate, Trithionate, and Thiosulfate in Alkaline Media. *Environ. Sci. Technol.* **1982**, *16* (12), 852−857.

(39) Schmid, D.; Karlström, O.; Kuvaja, V.; Vuorinen, I.; Paavola, M.; Hupa, M. Role of Sulfite Oxidation in NO2 Absorption in a PH-Neutral Scrubber Solution. *Energy Fuels* **2022**, *36* (5), 2666−2672.

(40) Gerding, H.; Eriks, K. The Raman Spectra of Di-Tri- and Tetrathionate Ions in Aqueous Solutions. *Recl. Trav. Chim. Pays-Bas.* **1950**, *69* (6), 724−728.

(41) Shi, M.; Ding, J.; Liu, X.; Zhong, Q. Mechanisms of Sulfite Oxidation in Sulfite-Nitrite Mixed Solutions. *Atmos. Pollut. Res.* **2019**, *10* (2), 412−417.